Applied Surface Science 401 (2017) 142–145

Contents lists available at ScienceDirect

Applied Surface Science

journal homepage: www.elsevier.com/locate/apsusc

Growth of layered superconductor β-$PdBi_2$ films using molecular beam epitaxy

N.V. Denisov[a,*], A.V. Matetskiy[a], A.V. Tupkalo[a], A.V. Zotov[a,b,c], A.A. Saranin[a,b]

[a] Institute of Automation and Control Processes FEB RAS, 5 Radio Street, 690041 Vladivostok, Russia
[b] School of Natural Sciences, Far Eastern Federal University, 690950 Vladivostok, Russia
[c] Department of Electronics, Vladivostok State University of Economics and Service, 690600 Vladivostok, Russia

ARTICLE INFO

Article history:
Received 29 September 2016
Received in revised form
28 December 2016
Accepted 31 December 2016
Available online 5 January 2017

Keywords:
Atom–solid interactions
Bismuth
Palladium
Superconductivity

ABSTRACT

Bulk β-$PdBi_2$ layered material exhibits advanced properties and is supposed to be probable topological superconductor. We present a method based on molecular beam epitaxy that allows us to grow β-$PdBi_2$ films from a single β-$PdBi_2$ triple layer up to the dozens of triple layers, using Bi(111) film on Si(111) as a template. The grown films demonstrate structural, electronic and superconducting properties similar to those of bulk β-$PdBi_2$ crystals. Ability to grow the β-$PdBi_2$ films of desired thickness opens the promising possibilities to explore fascinating properties of this advanced material.

1. Introduction

Layered materials (LMs) are built of neutral, single or several atom-thick layers of atoms featuring covalent or ionic connections within each layer without dangling bonds, whereas the layers are held together via van der Waals bonding along the third axis. Such materials were actively studied in the second half of the last century and were shown to exhibit a wide range of interesting properties including superconductivity and charge density waves [1,2]. Lately, discovery of graphene [3], topological nontrivial states in Bi_2Se_3 and Bi_2Te_3 [4,5] and general interest to low-dimensional materials lead to resurgence of interest in LMs. Due to their unique atomic structure some LMs could form stable isolated mono or multilayer sheets which was proven by exfoliation of one layer of MoS_2 [6] and other layered crystals. Moreover, studies of MoS_2 flakes of variable thickness showed that electronic properties change from indirect semiconductor in five or more layers to direct semiconductor in one layer of MoS_2 [7]. Such behavior was attributed to the weak van der Waals interlayer interaction affecting the band structure of this LM [8]. Dependence of properties on the number of layers was also detected in other layered crystals such as $NbSe_2$ [9], $TaSe_2$ [10], etc. As modulation of properties of LMs by changing number of layers is rather universal for these materials, LMs could provide endless variety of building blocks with finely tuned properties for novel electronic devices [11,12] and van der Waals heterostructures [13]. Unfortunately, despite some recent success in creation of LM films by chemical vapor deposition [14], molecular beam epitaxy (MBE) [15] and other methods [16] controllable growth for most of the LM films remains complex and poorly explored matter and exfoliation of bulk crystals remains the main method for obtaining LM films.

β-$PdBi_2$ is a superconductor LM which transition temperature equals 5.4 K [17–19]. In addition, β-$PdBi_2$ has recently been found to display nontrivial topological properties [20] and has been proposed to be probable topological superconductor. All the experimental data reported to date have been obtained with bulk crystals of β-$PdBi_2$ grown by "melt-growth" method at temperatures of about 900 °C. This method produces high-quality single crystals but is not viable for growth of films of controlled thickness. Molecular beam epitaxy (MBE) could provide a principal possibility to reach this goal. Bearing in mind also abilities for fabrication of various heterostructures or for exploring proximity effects using various substrates, one can consider MBE as the technique which provides an additional degree of freedom both for researches and applications.

To our knowledge, successful MBE growth of β-$PdBi_2$ thin films has been reported only in a very recent work by Lv et al. [21]. The authors used $SrTiO_3$(001) crystal as a substrate and characterized structure and superconducting properties using

* Corresponding author.
E-mail address: denisov@iacp.dvo.ru (N.V. Denisov).

http://dx.doi.org/10.1016/j.apsusc.2016.12.239
0169-4332/

scanning tunneling microscopy (STM) and low-temperature scanning tunneling spectroscopy (STS), respectively. Superconducting transition temperature was estimated to be 6.1 ± 0.4 K. The results of STS measurements were interpreted as providing an evidence for time-reversal symmetry protected nontrivial nature of topological superconductivity and occurrence of Majorana zero modes [21].

In the present paper, we report on the MBE growth of β-$PdBi_2$ thin films with a thickness control from one to dozens layers using deposition of Pd and Bi onto the Bi(111) film grown on Si(111). Structural analysis of the grown β-$PdBi_2$ film was conducted using low energy electron diffraction (LEED) and scanning tunneling microscopy. Electronic properties were examined by angular-resolved photoemission spectroscopy (ARPES). Transport properties were measured *ex situ* using van der Pauw method with cooling the sample to liquid-He temperatures. The obtained results demonstrate that the grown films exhibit the structure and electronic properties that coincide with the known data for the bulk β-$PdBi_2$ crystals. The films occur in three domain orientations and demonstrate a superconducting transition at 3.1 K.

2. Experiment

Growth of the films followed by STM and LEED observations were carried out in the Omicron STM Compact Lab system operated in an ultrahigh vacuum ($\sim 7 \times 10^{-11}$ Torr). All STM images were acquired in a constant-current mode at room temperature. ARPES experiments were performed with an Omicron MULTIPROBE ARPES system operated in an ultrahigh vacuum (10^{-10} Torr). To transfer the samples to the ARPES system we used evacuated transfer unit. The ARPES measurements were conducted using a hemispherical electron analyzer VG Scienta R3000. The light source was a high-flux monochromatized He discharge lamp with a photon energy of 21.2 eV. The low-temperature transport measurements of the grown $PdBi_2$ films were conducted in the Oxford Instruments TeslatronPT system.

Atomically-clean Si(111)7×7 surfaces were prepared *in situ* by flashing samples to 1280 °C after they were outgassed at ~600 °C for several hours. Bi(111) surface was prepared by growing 20 bi-layers of Bi on Si(111)7×7 surface [22]. Bismuth was deposited from a commercial HTEZ40 cell, deposition rate of Bi being calibrated using Si(111)$\beta - \sqrt{3} \times \sqrt{3}$-Bi surface as a reference [23]. Palladium was deposited from a filament evaporation unit at a rate of 0.2 ML/min. (where 1 ML (monolayer) = 8.98×10^{14} atoms/cm^2 for 3.34 Å square lattice). Deposition rate of Pd was calibrated using the Si(111)$\sqrt{3} \times \sqrt{3}$-Pd surface reconstruction [24] as a reference.

3. Results and discussion

Remind that the β-$PdBi_2$ is layered material with tetragonal structure, I4/mmm space group. Electrically neutral layers consist of atomic layer of Pd sandwiched between two atomic layers of Bi, such a structure is defined as a triple layer (TL). The TLs are packed alternately and form the body centered tetragonal unit cell with parameters $a = b = 3.36$ Å and $c = 12.98$ Å, as shown in Fig. 1(a). The spacing between the TLs is rather large, with interlayer Bi–Bi distance being ~3.8 Å, indicating that the TLs are bonded to each other by weak van der Waals forces.

Adsorption of Pd onto Bi(111) at RT results in the formation of a single TL of β-$PdBi_2$, which structure and composition were verified using LEED and STM observations. In the LEED pattern obtained after deposition of Pd onto Bi(111) [Fig. 1(b) and (c)] one can see superposition of the spots from Bi(111)1×1 surface having hexagonal symmetry (indicated by open black circles in Fig. 1(c)) and those from three domains having square symmetry (indicated by red, yellow and green open circles in Fig. 1(c)) rotated by 15° relative to the Bi(111) main directions and 120° relative to each other. The square lattice constant deduced from the LEED pattern equals 3.4 Å which value matches properly the unit cell parameter of β-$PdBi_2$ (001)1×1 surface [Fig. 1(a)]. STM observations demonstrate that after depositing 1.0 ML Pd up to 85% of the surface area is occupied by the square-lattice structure [Fig. 1(d)] indicating that this is plausibly a single TL of β-$PdBi_2$. Occurrence of three rotational β-$PdBi_2$ domains is a natural sequence of the threefold symmetry of the underlying Bi(111) surface. Another consequence of superposing of the film on a substrate of a different symmetry is developing of the Moiré pattern of meandering bright and dim rows in the [110] direction of the β-$PdBi_2$ lattice. It is worth noting that the Moiré pattern is absent in the next β-$PdBi_2$ layers [see the inset in Fig. 2(a)].

Pd adsorption beyond 1 ML leads to the growth of three-dimensional Pd islands on the β-$PdBi_2$ TL surface. Thus, one can conclude that single β-$PdBi_2$ TL acts as a blocking layer which prevents reaction of excessive Pd with Bi. In order to grow β-$PdBi_2$ films beyond the first TL, one has to use co-deposition of Pd and Bi with a stoichiometric ratio of 1:2, the growth temperature being still kept at RT and the growth rate was ~0.2 TL/min. Growth of the β-$PdBi_2$ films up to dozens of TLs proceeds almost in a layer-by-layer fashion. As an example, Fig. 2 presents the LEED and STM data for the 10-TL β-$PdBi_2$ film. In particular, the LEED pattern [Fig. 2(b)] demonstrates that that there are no surface structures other than those of the β-$PdBi_2$ film in three domain orientations. STM observations [Fig. 2(a) and (c)] demonstrates the layer-by-layer growth with the step height being ~6.5 Å, that coincides with the thickness

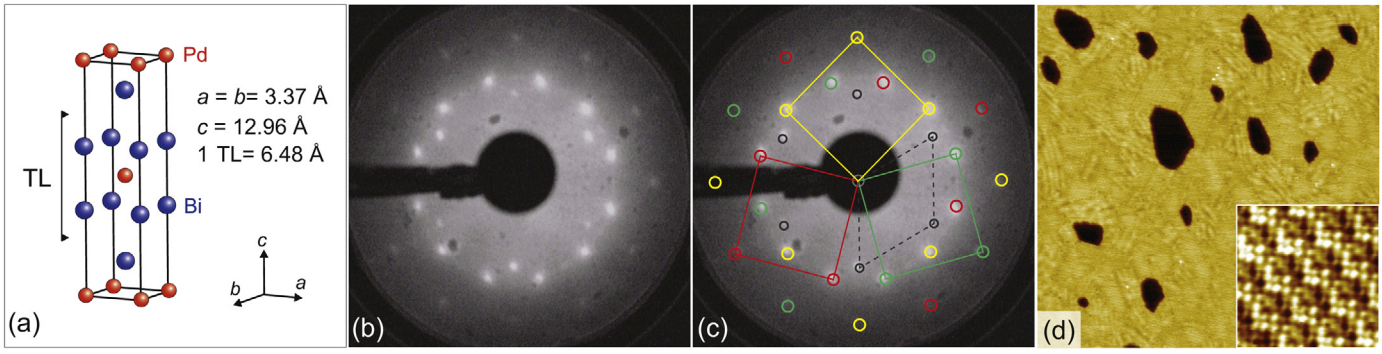

Fig. 1. (a) Schematic crystal structure of β-$PdBi_2$. (b) LEED pattern ($E_p = 70$ eV) of the incomplete 1-TL-thick β-$PdBi_2$ film grown on Bi(111). (c) Interpretation of the LEED pattern shown in (b) where Bi(111) spots are indicated by open black circles and spots of the three β-$PdBi_2$ domains by green, yellow and red open circles. The structure unit cells are outlined by the solid lines of corresponding color. (d) 120×120 nm^2 STM image of the incomplete 1-TL-thick β-$PdBi_2$ film on Bi(111) where dark patches correspond to the bare Bi(111) surface. Inset in (d) presents an enlarged 5×5 nm^2 fragment of the β-$PdBi_2$ film to show the Moiré pattern developed at the surface. (For interpretation of the references to color in this figure legend, the reader is referred to the web version of the article.)

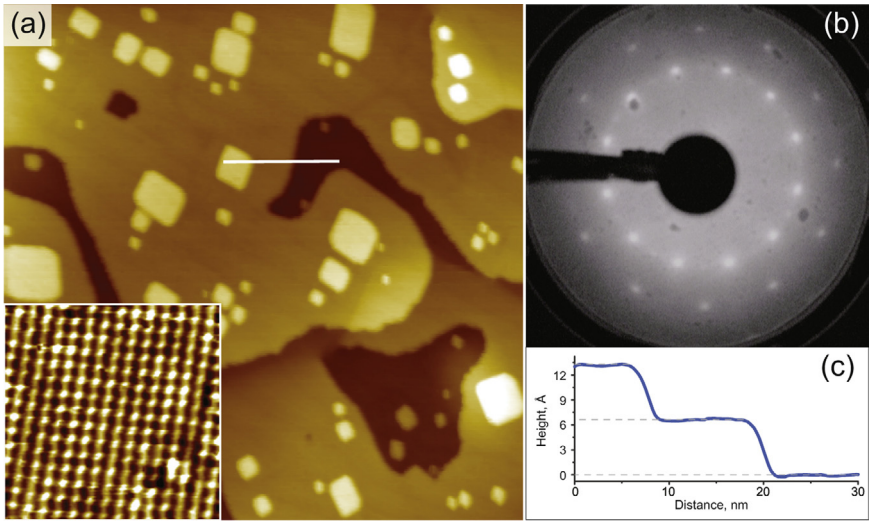

Fig. 2. (a) 150 × 150 nm^2 STM image and (b) corresponding LEED pattern (E_p = 70 eV) from the 10-TL β-$PdBi_2$ film. Inset in (a) shows the enlarges 5 × 5 nm^2 fragment of the surface. (c) STM line profile along the white line in (a).

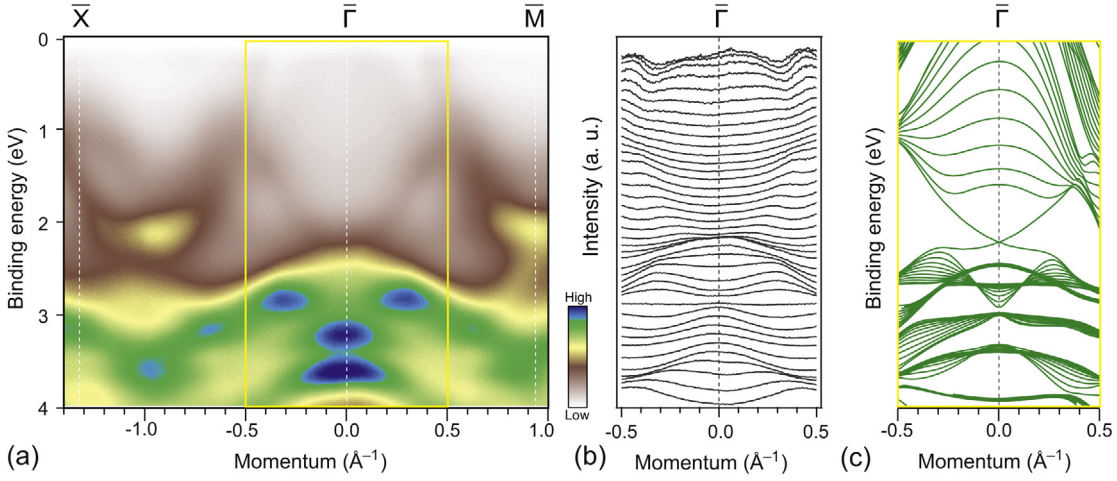

Fig. 3. (a) Experimental ARPES spectrum recorded along the $\bar{X}$–$\bar{\Gamma}$ and $\bar{\Gamma}$–$\bar{M}$ directions from the 10-TL β-$PdBi_2$ film. (b) Momentum distribution curves in the spectral region outlined in (a) by a yellow frame. (c) Calculated surface band dispersions for the bulk β-$PdBi_2$ taken from Ref. [20] for the same spectral region. (For interpretation of the references to color in this figure legend, the reader is referred to the web version of the article.)

of the single β-$PdBi_2$ TL. Note that this differs from the β-$PdBi_2$ growth on $SrTiO_3$(001) substrate where the growth proceeds via Volmer–Weber mode [21].

Angle-resolved photoemission spectrum acquired from the 10-TL β-$PdBi_2$ film and corresponding momentum distribution curves of its fragment within a yellow frame are shown in Fig. 3(a) and (b), respectively. One can see that they are in a good agreement with spectrum calculated for the bulk β-$PdBi_2$ crystal in [20]. Unfortunately, due to the three-domain occurrence of the β-$PdBi_2$ film in our experiment, comparison is viable only for electron states near the $\bar{\Gamma}$ point, as the states near the $\bar{M}$ and $\bar{X}$ points are mixed. Nevertheless, all the bulk bands and the band attributed to nontrivial topology of β-$PdBi_2$ [20] are clearly seen, indicating that the film has a similar electron band structure as the bulk crystals.

The temperature dependence of electrical resistivity ρ for the 10-TL β-$PdBi_2$ film is shown in Fig. 4. One can see a clear transition to the superconducting state at critical temperature T_c = 3.1 K. For comparison, the critical temperature for a bulk β-$PdBi_2$ crystal was found in early studies as being 4.25 K [25]. However, it has recently been reconsidered to be equal to 5.4 K [17–19]. The increase in critical temperature was attributed to a higher quality of the β-$PdBi_2$

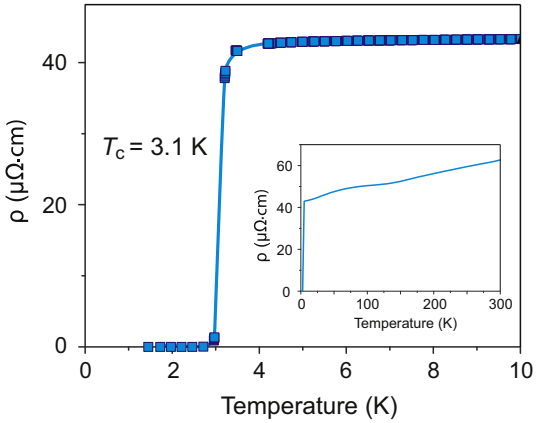

Fig. 4. Temperature dependence of the electrical resistivity ρ of the 10-TL β-$PdBi_2$ film in the temperature range of 0–10 K and 0–300 K (in the inset).

crystals. Lv et al. [21] reported even higher critical temperature of 6.1 K for β-$PdBi_2$ films grown on $SrTiO_3$(001). The value obtained in the present work for the β-$PdBi_2$ films on Bi(111)/Si(111) is lower than all these values. There are several possible reasons for lowering the critical temperature. First, it is a general trend that a critical temperature for thin films is often lower than that for the bulk of the same material. Second, occurring of three domains in the present β-$PdBi_2$ films means reducing crystalline quality which might hamper the superconductivity. A modest crystal quality of the film is reflected also in the relatively low residual resistivity ratio [RRR, $\rho(T = 300\,K)/\rho(T = T_c)$] of ~1.5. For comparison, for the high-quality bulk β-$PdBi_2$ crystal RRR is reported to be about 12 [17]. Third, while exposing the sample to air ambient for the transport measurements the thin β-$PdBi_2$ film might adsorb contaminations that can reduce the critical temperature. A similar effect was reported for the β-$PdBi_2$ crystals doped with different species (e.g., Pb and Na) [19]. Fourth, surface stress due the lattice mismatch between β-$PdBi_2$ film and Bi(111)/Si(111) substrate might also be the reason, bearing in mind that high pressure is known to suppresses the critical temperature of β-$PdBi_2$ crystal [19]. We believe that experiments on exploring superconducting properties of the β-$PdBi_2$ of the various thicknesses conducted without breaking vacuum between film growth and transport measurements could make a proper choice among the possibilities listed above. In addition, available data set on β-$PdBi_2$ film growth given in [21] and present paper can serve as a useful base for the prospective investigations of this advanced layered material.

4. Conclusions

In conclusion, we present here an MBE-related method to grow β-$PdBi_2$ films of the desired thickness starting from a single triple layer. The Bi(111) film grown on Si(111) surface has been found to be an appropriate template for the β-$PdBi_2$ film growth. The β-$PdBi_2$ film grows in layer-by-layer fashion in three domain orientations which make angle of 15° with the main crystallographic directions of Bi(111) and 120° between domains. ARPES measurements reveal that an electron band structure of the film is the same as that of the bulk β-$PdBi_2$ crystals. The 10-TL β-$PdBi_2$ film was found to become a superconductor at the critical temperature of 3.1 K. Ability of growing β-$PdBi_2$ films of any desirable thickness using MBE adds a new degree of freedom in exploration of advanced properties of the β-$PdBi_2$ material. In particular, thickness dependence of electronic band structure and superconducting characteristics can be studied. Another promising direction of investigations is related to the growth of β-$PdBi_2$ films with modulated doping and growth of the heterostructures incorporating β-$PdBi_2$ and other layered materials. Using various substrates, proximity effects on superconducting properties can also be addressed.

Acknowledgements

The present work was supported in part by the Grants NSh-6889.2016.2 and MK-5560.2016.2 of the President of the Russian Federation, 16-02-00505 of the Russian Foundation for Basic Researches, and 15-I-4-012 (0262-2015-0131) of the Russian Academy of Sciences Program “Far East”. Technical assistance of E. Yu. Subbotin in conductivity measurements are greatly acknowledged.

References

[1] R.C. Morris, Connection between charge-density waves and superconductivity in $NbSe_2$, Phys. Rev. Lett. 34 (1975) 1164.
[2] J. Wilson, F. Disalvo, S. Mahajan, Charge-density waves and superlattices in metallic layered transition-metal dichalcogenides, Adv. Phys. 24 (2001) 1171.
[3] K.S. Novoselov, D. Jiang, F. Schedin, T.J. Booth, V.V. Khotkevich, S.V. Morozov, A.K. Geim, Two-dimensional atomic crystals, Proc. Natl. Acad. Sci. U. S. A. 102 (2005) 10451.
[4] H. Zhang, C.-X. Liu, X.-L. Qi, X. Dai, Z. Fang, S.-C. Zhang, Topological insulators in Bi_2Se_3, Bi_2Te_3 and Sb_2Te_3 with a single Dirac cone on the surface, Nat. Phys. 5 (2009) 438.
[5] Y. Xia, D. Qian, D. Hsieh, L. Wray, A. Pal, H. Lin, A. Bansil, D. Grauer, Y.S. Hor, R.J. Cava, M.Z. Hasan, Observation of a large-gap topological-insulator class with a single Dirac cone on the surface, Nat. Phys. 5 (2009) 18.
[6] P. Joensen, R.F. Frindt, S.R. Morrison, Single-layer MoS_2, Mater. Res. Bull. 21 (1986) 457.
[7] K.F. Mak, C. Lee, J. Hone, J. Shan, T.F. Heinz, Atomically thin MoS_2: a new direct-gap semiconductor, Phys. Rev. Lett. 105 (2010) 136805.
[8] S.W. Han, H. Kwon, S.K. Kim, S. Ryu, W.S. Yun, D.H. Kim, J.H. Hwang, J.S. Kang, J. Baik, H.J. Shin, S.C. Hong, Band-gap transition induced by interlayer van der Waals interaction in MoS_2, Phys. Rev. B 84 (2011) 045409.
[9] N.E. Staley, J. Wu, P. Eklund, Y. Liu, L. Li, Z. Xu, Electric field effect on superconductivity in atomically thin flakes of $NbSe_2$, Phys. Rev. B 80 (2009) 184505.
[10] J.A. Galvis, P. Rodière, I. Guillamon, M.R. Osorio, J.G. Rodrigo, L. Cario, E. Navarro-Moratalla, E. Coronado, S. Vieira, H. Suderow, Scanning tunneling measurements of layers of superconducting 2H-$TaSe_2$: evidence for a zero-bias anomaly in single layers, Phys. Rev. B 87 (2013) 094502.
[11] H.S. Lee, S.-W. Min, Y.-G. Chang, M.K. Park, T. Nam, H. Kim, J.H. Kim, S. Ryu, S. Im, MoS_2 nanosheet phototransistors with thickness-modulated optical energy gap, Nano Lett. 12 (2012) 3695.
[12] Y.T. Lee, D.K. Hwang, S. Im, High-performance a MoS_2 nanosheet-based nonvolatile memory transistor with a ferroelectric polymer and graphene source-drain electrode, J. Korean Phys. Soc. 67 (2015) L1499.
[13] A.K. Geim, I.V. Grigorieva, Van der Waals heterostructures, Nature 499 (2013) 419.
[14] S. Najmaei, Z. Liu, W. Zhou, X. Zou, G. Shi, S. Lei, B.I. Yakodson, J.-C. Idrobo, P.M. Ajayan, J. Lou, Vapor phase growth and grain boundary structure of molybdenum disulfide atomic layers, Nat. Mater. 12 (2013) 754.
[15] G. Zhang, H. Qin, J. Teng, J. Guo, Q. Guo, X. Dai, Z. Fang, K. Wu, Quintuple-layer epitaxy of thin films of topological insulator Bi_2Se_3, Appl. Phys. Lett. 95 (2009) 053114.
[16] R. Lv, J.A. Robinson, R.E. Schaak, D. Sun, Y. Sun, T.E. Mallouk, M. Terrones, Transition metal dichalcogenides and beyond: synthesis, properties, and applications of single- and few-layer nanosheets, Acc. Chem. Res. 48 (2015) 56.
[17] Y. Imai, F. Nabeshima, T. Yoshinaka, K. Miyatani, R. Kondo, S. Komiya, I. Tsukada, A. Maeda, Superconductivity at 5.4 K in β-Bi_2Pd, J. Phys. Soc. Jpn. 81 (2012) 113708.
[18] E. Herrera, I. Guillamón, J.A. Galvis, A. Correa, A. Fente, R.F. Luccas, F.J. Mompean, M. García-Hernández, S. Vieira, J.P. Brison, H. Suderow, Magnetic field dependence of the density of states in the multiband superconductor β-Bi_2Pd, Phys. Rev. B 92 (2015) 054507.
[19] K. Zhao, B. Lv, Y.-Y. Xue, X.-Y. Zhu, L.Z. Deng, Z. Wu, C.W. Chu, Chemical doping and high-pressure studies of layered β-$PdBi_2$ single crystals, Phys. Rev. B 92 (2015) 174404.
[20] M. Sakano, K. Okawa, M. Kanou, H. Sanjo, T. Okuda, T. Sasagawa, K. Ishizaka, Topologically protected surface states in a centrosymmetric superconductor β-$PdBi_2$, Nat. Commun. 6 (2015) 8595.
[21] Y.-F. Lv, W.-L. Wang, Y.-M. Zhang, H. Ding, W. Li, L. Wang, K. He, C.-L. Song, X.-C. Ma, Q.-K. Xue, Experimental observation of topological superconductivity and Majorana zero modes on β-Bi_2Pd thin films, ArXiv:1607.07551.
[22] T. Nagao, J.T. Sadowski, M. Saito, S. Yaginuma, Y. Fujikawa, T. Kogure, T. Ohno, Y. Hasegawa, S. Hasegawa, T. Sakurai, Nanofilm allotrope and phase transformation of ultrathin Bi film on Si(111)-7 × 7, Phys. Rev. Lett. 93 (2004) 105501.
[23] T. Kuzumaki, T. Shirasawa, S. Mizuno, N. Ueno, H. Tochihara, K. Sakamoto, Re-investigation of the Bi-induced Si(111)-($\sqrt{3} \times \sqrt{3}$) surfaces by low-energy electron diffraction, Surf. Sci. 694 (2010) 1044.
[24] Y. Yabuuchi, F. Shoji, K. Oura, T. Hanawa, Y. Kishikawa, S. Okada, New surface structure of Pd on Si(111) studied by low-energy ion-scattering spectroscopy and LEED-AES, Jpn. J. Appl. Phys. 21 (1982) L752.
[25] N.N. Zhuravlev, Structure of superconductors. X. Thermal, microscopic, and X-ray investigation of the bismuth-palladium system, Sov. Phys. JETP 5 (1957) 1064.